Adaptive Robust Control for Servo Mechanisms With Partially Unknown States via Dynamic Surface Control Approach

Guozhu Zhang, Jie Chen, *Member, IEEE*, and Zhiping Lee

***Abstract*—In order to achieve high performance control for servo mechanisms with electrical dynamics and unmeasurable states, an observer-based adaptive robust controller (ARC) is developed via dynamic surface control (DSC) technique. To represent electrical dynamics, a third-order model is used to describe the servo mechanism. However, the third-order model brings some difficulties to observer construction and recursive controller design. To solve this problem, we first transform the model into a particular form suitable for observer design, and then construct a parameterized observer to estimate the unmeasurable states. The state estimation is based on the output and its derivatives, which can be acquired by an output differential observer. Subsequently, an observer-based ARC can be developed through DSC technique, with which the problem of "explosion of complexity" caused by backstepping method in the traditional ARC design can be overcome. A stability analysis is given, showing that our control law can guarantee uniformly ultimate boundedness of the solution of the closed-loop system, and make the tracking error arbitrarily small. This scheme is implemented on a precision two-axis turntable. Experimental results are presented to illustrate the effectiveness and the achievable control performance of the proposed scheme.**

***Index Terms*—Adaptive robust control (ARC), dynamic surface control (DSC), servo mechanism, state observer, two-axis turntable.**

I. INTRODUCTION

THE PERFORMANCE of servo mechanisms is frequently deteriorated by external disturbances and nonlinearities (e.g., friction and cogging force). Moreover, there must be some parametric uncertainties in the plant model due to unavoidable modeling errors. When designing controllers for servo mechanisms, all the factors mentioned above (i.e., disturbances, nonlinearities and parametric uncertainties) need considering.

Adaptive robust control (ARC) proposed by Yao and Tomizuka in [1] and [2] combines the advantages of adaptive control [3] and deterministic robust control (DRC) [4] and overcomes their practical performance limitations for a reasonably large class of nonlinear systems [5]. It has been proved that for the semi-strict feedback nonlinear systems, the ARC is not only able to attenuate the influence of disturbances and nonlinearities, but also to achieve asymptotic output tracking in the presence of parametric uncertainties only [1]. In [6], ARC is successfully applied to a third order servo mechanism, but its control law is state dependent.

In some cases, partial states of the plant such as motor current and angular velocity are unmeasurable, so that state feedback control laws will not be applicable. To solve this problem, the observer-based output feedback ARC is developed in [16] and [20] by combining state observer with ARC design. Several applications of the output feedback ARC have been reported. In [7], an output feedback ARC is developed for a magnetic levitation system. In [8], the observer-based output feedback ARC is utilized to an epoxy core linear motor whose current dynamics is negligible. However, these results are merely applicable to the plants with second-order model, whose structure is suitable for the observer design. The ordinary third-order models of servo mechanisms with current dynamics may lead to some difficulties in the observer design. To this issue, a novel model transformation that facilitates the observer construction is proposed in this paper.

Additionally, the commonly used backstepping technique in traditional ARC design may result in the problem of "explosion of complexity", especially for the plant with order larger than three [9], [10]. As shown in [6], the state feedback ARC developed by backstepping approach for a third-order plant is already quite complicated. If an observer-based ARC is designed, the computation will be more cumbersome. To eliminate "explosion of complexity" in backstepping design, the dynamic surface control (DSC) method was proposed [10]. The DSC approach replaces the derivatives at each step of the traditional backstepping design by some first order filters. Because of its convenience, the DSC technique has been used in adaptive controller design [11], [12] and state feedback ARC design [13]. In this paper, we use DSC technique to simplify the design of an observer-based ARC, which is more complicated than the adaptive controller and state feedback ARC when synthesized by integrator backstepping approach.

In this paper, the servo mechanisms with current dynamics and partially unknown states are under investigation. The model of the servo mechanism is first transformed into a particular form suitable for observer design, and then a state observer is designed so that the unknown states can be replaced by their estimates. Finally, the DSC technique is used to design the adaptive robust controller.

This paper is organized as follows. Dynamic model of the servo mechanisms and problem formulation are presented in Section II. The proposed ARC controller is shown in Section III. The closed-loop system stability is analyzed in Section IV. Experimental results are presented in Section V and conclusions are drawn in Section VI.

Manuscript received November 24, 2008; revised March 16, 2009. Manuscript received in final form June 05, 2009. First published August 18, 2009; current version published April 23, 2010. Recommended by Associate Editor Z. Wang.

The authors are with the Department of Automatic Control, Beijing Institute of Technology, Beijing 100081, China (e-mail: zhangguozhu_bit@yahoo.com.cn; chenjie@bit.edu.cn; dynebit@yahoo.com.cn).

Color versions of one or more of the figures in this paper are available online at http://ieeexplore.ieee.org.

Digital Object Identifier 10.1109/TCST.2009.2025265

II. Dynamic Models and Problem Formulation

A. Dynamic Models of Servo Mechanisms

The dynamics of a dc motor servo mechanism can be described as [6], [8]

$$J\ddot{q} = T_m - B\dot{q} - T_{\text{friction}}(\dot{q}) - T_{\text{dis}} \tag{1}$$

where J is the inertial sum of load and armature, q is the motor's output angle, T_m is the electromagnetic torque, T_{friction} is the friction torque, T_{dis} is the disturbance torque, B is the viscous friction coefficient. In general, T_{friction} is considered to have the following form [14]:

$$T_{\text{friction}}(\dot{q}) = \left[T_c + (T_s - T_c)e^{-|\dot{q}/\dot{q}_s|^{\xi}}\right]\operatorname{sgn}(\dot{q}). \tag{2}$$

In the equation, T_s is the level of the static friction torque, T_c is the minimum level of Column friction torque, and $\dot{q}_s$ and ξ are empirical parameters used to describe the Stribeck effect. A popular simplified model that relates the electromagnetic torque T_m to the input voltage u is given by [15]

$$T_m = K_F i, \quad L di/dt + iR + K_E\dot{q} = u \tag{3}$$

where R and L are the resistance and induction of the armature, respectively, i is the motor current, u is the input voltage, K_F is the force constant, K_E is the electromotive force coefficient. Defining the angle, angular velocity, and current as the state variables, i.e., $[x_{10}, x_{20}, x_{30}]^T = [q, \dot{q}, i]^T$, from (1)–(3), the entire system can be expressed in the state space form as

$$\begin{cases} \dot{x}_{10} = x_{20} \\ \dot{x}_{20} = \frac{1}{J}\left[K_F x_{30} - Bx_{20} - T_{\text{friction}}(x_{20}) - T_{dis}\right] \\ \dot{x}_{30} = -\frac{R}{L}x_{30} - \frac{K_E}{L}x_{20} + \frac{1}{L}u. \end{cases} \tag{4}$$

In this paper, we assume that the state x_{10} is measureable, while x_{20} and x_{30} (i.e., the angular velocity and current of the servo mechanism) are unmeasureable. In order to linearly parameterize model (4), the friction torque T_{friction} is approximated by the quantity $\theta_f S_f$, where S_f is chosen as the following differentiable function [8], [21]:

$$S_f = (2/\pi)\arctan(K_s x_2), \quad K_s > 0. \tag{5}$$

The parameter K_s in (5) should be chosen to be a large positive number, so that the smooth function $\theta_f S_f$ can approximate T_{friction} with adequately small residual error. The approximating error of $\theta_f S_f$ is $d = T_{\text{friction}} - \theta_f S_f$. Substituting (5) into (4), we have

$$\begin{cases} \dot{x}_{10} = x_{20} \\ \dot{x}_{20} = -\theta_{10}x_{20} + \theta_{20}x_{30} - \theta_{30}S_f(x_{20}) + \Delta \\ \dot{x}_{30} = -\theta_{40}x_{20} - \theta_{50}x_{30} + \theta_{60}u \end{cases} \tag{6}$$

where $\Delta = (-T_{\text{dis}} - d)/J$. The definition of θ_{i0} $(i = 1, \ldots, 6)$ is as follows:

$$\theta_{10} = \frac{B}{J};\ \theta_{20} = \frac{K_F}{J};\ \theta_{30} = \frac{\theta_f}{J};\ \theta_{40} = \frac{K_E}{L};\ \theta_{50} = \frac{R}{L};\ \theta_{60} = \frac{1}{L}.$$

B. Assumptions and Problem Statement

For simplicity, the following notations will be used: $\bullet_i$ for the ith component of the vector $\bullet$, $\bullet_{\min}$ for the minimum value of $\bullet$, and $\bullet_{\max}$ for the maximum value of $\bullet$. The operation $\leq$ for two vectors is performed in terms of the corresponding elements of the vectors.

In general, the parameters of the model cannot be accurately determined. Thus, we assume, in this paper, that the uncertain parameters are in certain known intervals, as shown in assumption 1 and assumption 2. In addition, assumption 3 is made for the desired motion trajectory $x_{1d}(t)$.

Assumption 1: $\theta_{i0} \in [\theta_{i0\min}, \theta_{i0\max}]$, moreover $\theta_{i0\min}$ and $\theta_{i0\max}$ are known.

Assumption 2: The disturbance Δ is bounded, i.e., $|\Delta| < \delta$.

Assumption 3: The desired trajectory are continuous and available, and $[x_{1d}, \dot{x}_{1d}, \ddot{x}_{1d}]^T \in \Omega_d$ with known compact set $\Omega_d = \{[x_{1d}, \dot{x}_{1d}, \ddot{x}_{1d}]^{\mathrm{T}} : x_{1d}^2 + \dot{x}_{1d}^2 + \ddot{x}_{1d}^2 \leq B_0\} \subset R^3$, whose size B_0 is a known positive constant.

The control problem of this paper can be stated as follows: given the desired motion trajectory $x_{1d}(t)$, the objective is to synthesize a control input u such that the output $y = x_{10}$ tracks $x_{1d}(t)$ as closely as possible in spite of various model uncertainties. Since the servo mechanisms studied in this paper have partially unknown states, it is necessary to design controllers which are only dependent on the available states.

III. Adaptive Robust Control With Partial States Feedback

The method proposed in this paper is motivated by the observer-based ARC developed in [16] and the ARC design via DSC technique presented in [13]. In order to reduce the dynamic uncertainties caused by the unmeasurable states, we first transform the model into a particular form, and then develop a parameterized observer to estimate the unavailable states. Afterward, an adaptive robust controller relying on the available states and estimates of the unavailable states is synthesized by DSC technique. Owning to the DSC approach, the explosion of complexity in traditional backstepping design is avoided, and then the proposed controller is less complicated than that developed by backstepping as in [1].

A. Model Normalization

In order to design a parameterized observer, we transform model (6) into a normalized form. From the second equation of (6), we have

$$\theta_{20}x_{30} = \theta_{10}x_{20} + \theta_{30}S_f(x_{20}) + \dot{x}_{20} - \Delta. \tag{7}$$

Substituting (7) into the third equation of (6), we obtain

$$\begin{cases} \dot{x}_1 = x_2 \\ \dot{x}_2 = -\theta_1 x_2 + x_3 - \theta_2 S_f(x_2) + \Delta_1 \\ \dot{x}_3 = -\theta_3 x_2 - \theta_4\dot{x}_2 - \theta_5 S_f(x_2) + \theta_6 u + \Delta_2 \end{cases} \tag{8}$$

where

$$x_1 = x_{10},\ x_2 = x_{20},\ x_3 = x_{30}\theta_{20} \tag{9}$$

and

$$\begin{cases} \Delta_1 = \Delta,\ \Delta_2 = \Delta\theta_{50}, \theta_1 = \theta_{10} = \frac{B}{J} \\ \theta_2 = \theta_{30} = \frac{\theta_f}{J},\ \theta_3 = \theta_{10}\theta_{50} + \theta_{20}\theta_{40} = \frac{BR+K_F K_E}{JL} \\ \theta_4 = \theta_{50} = \frac{R}{L},\ \theta_5 = \theta_{30}\theta_{50} = \frac{\theta_f R}{JL},\ \theta_6 = \theta_{20}\theta_{60} = \frac{K_F}{JL}. \end{cases} \tag{10}$$

According to (10) and assumption 1, there exist $\theta_{i\min}$ and $\theta_{i\max}$ satisfying $\theta_i \in [\theta_{i\min}, \theta_{i\max}]$, $(i = 1, \ldots, 6)$. Furthermore, $\theta_{i\min}$ and $\theta_{i\max}$ are functions of $\theta_{i0\min}$ and $\theta_{i0\max}$. From assumption 2 and the boundedness of θ_{i0}, it can be seen that Δ_1 and Δ_2 are also bounded. Therefore, model (8) has the following properties.

Property 1: $\theta_i \in [\theta_{i\min}, \theta_{i\max}]$, $(i = 1, \ldots, 6)$, where $\theta_{i\min}$ and $\theta_{i\max}$ are known.

Property 2: $|\Delta_1| \leq \delta_1$, $|\Delta_2| \leq \delta_2$, where δ_1 and δ_2 are known.

B. Discontinuous Projection

Define the unknown parameter set θ as $\theta = [\theta_1, \theta_2, \theta_3, \theta_4, \theta_5, \theta_6]^T \in \Re^6$. Let $\hat{\theta}$ denote the estimate of θ and $\tilde{\theta}$ represent the estimation error (i.e., $\tilde{\theta} = \hat{\theta} - \theta$). The discontinuous projection operator is defined as [17]

$$\mathrm{Proj}_{\hat{\theta}}(\bullet) = \begin{cases} 0, & \text{if } \hat{\theta}_i = \theta_{i\max} \text{ and } \bullet > 0 \\ 0, & \text{if } \hat{\theta}_i = \theta_{i\min} \text{ and } \bullet < 0 \\ \bullet, & \text{otherwise.} \end{cases} \tag{11}$$

If the adaptation law is given by $\dot{\hat{\theta}} = \mathrm{Proj}_{\hat{\theta}}(\Gamma\tau)$, where Γ is a diagonal positive definite matrix, then for any adaptation function τ, the projection mapping used in (11) assures [18].

P1 If $\hat{\theta}(0) \in \Omega_\theta$, then

$$\hat{\theta} \in \Omega_\theta := \{\hat{\theta} : \theta_{\min} \leq \hat{\theta} \leq \theta_{\max}\} \tag{12}$$

where $\theta_{\min} = [\theta_{1\min}, \ldots, \theta_{6\min}]^T$ and $\theta_{\max} = [\theta_{1\max}, \ldots, \theta_{6\max}]^T$.

P2

$$\tilde{\theta}^T \left(\Gamma^{-1}\mathrm{Proj}_{\hat{\theta}}(\Gamma\tau) - \tau\right) \leq 0, \quad \forall\tau. \tag{13}$$

C. Design of the State Observer

The last two equations of model (8) can be rewritten as

$$\begin{aligned} \dot{\bar{x}} = A_0\bar{x} + (k - e_1\theta_1 - e_2\theta_3)x_2 - (e_1\theta_2 + e_2\theta_5)S_f(x_2) \\ - e_2\theta_4\dot{x}_2 + e_2\theta_6 u + \begin{bmatrix}\Delta_1 \\ \Delta_2\end{bmatrix} \end{aligned} \tag{14}$$

where $\bar{x} = [x_2, x_3]^T$, $e_1 = [1, 0]^T$, $k = [k_1, k_2]^T$, and

$$A_0 = \begin{bmatrix} -k_1 & 1 \\ -k_2 & 0 \end{bmatrix}.$$

Then, by suitably choosing k, one can synthesize the observer matrix A_0 with arbitrarily fast convergence rate. Thus, there exists a symmetric positive definite matrix P such that $PA_0 + A_0^T P = -I$, $P = P^T > 0$. Following the design procedure of [3], one can define the following K-filters:

$$\begin{cases} \dot{\xi}_0 = A_0\xi_0 + kx_2; \dot{\xi}_1 = A_0\xi_1 - e_1 x_2; \\ \dot{\xi}_2 = A_0\xi_2 - e_1 S_f(x_2); \dot{\xi}_3 = A_0\xi_3 - e_2 x_2; \\ \dot{\xi}_4 = A_0\xi_4 - e_2\dot{x}_2; \dot{\xi}_5 = A_0\xi_5 - e_2 S_f(x_2); \\ \dot{\xi}_6 = A_0\xi_6 + e_2 u. \end{cases}$$

According to the above equations, since $e_1 x_2 = A_0 e_2 x_2$, $kx_2 = k_1 e_1 x_2 + k_2 e_2 x_2$, and $e_1 S_f = A_0 e_2 S_f$, we know that ξ_1, ξ_2 and ξ_4 can be computed in the way described below:

$$\xi_1 = A_0\xi_3;\ \xi_0 = -k_1\xi_1 - k_2\xi_3;\ \xi_2 = A_0\xi_5.$$

Therefore, the K-filters can be simplified as

$$\begin{cases} \dot{\xi}_3 = A_0\xi_3 - e_2 x_2; \dot{\xi}_4 = A_0\xi_4 - e_2\dot{x}_2; \\ \dot{\xi}_5 = A_0\xi_5 - e_2 S_f(x_2); \dot{\xi}_6 = A_0\xi_6 + e_2 u; \\ \xi_1 = A_0\xi_3; \xi_0 = -k_1\xi_1 - k_2\xi_3; \xi_2 = A_0\xi_5; \\ \hat{\bar{x}} = \xi_0 + \sum_{i=1}^{6} \theta_i\xi_i. \end{cases} \tag{15}$$

Then, the states of (14) can be rewritten as

$$\bar{x} = \xi_0 + \sum_{i=1}^{6} \theta_i\xi_i + \varepsilon_x \tag{16}$$

where ε_x is the estimation error. From (14) and (16) we know that $\dot{\varepsilon}_x = A_0\varepsilon_x + [\Delta_1, \Delta_2]^T$. The solution of this equation is

$$\varepsilon_x = \varepsilon_0 + \varepsilon_\Delta \tag{17}$$

where ε_0 is the zero input response of equation $\dot{\varepsilon}_0 = A_0\varepsilon_0$ and $\varepsilon_\Delta = \int_0^t e^{A_0(t-\tau)}[\Delta_1, \Delta_2]^T d\tau$ for $t \geq 0$. Noting property 2 and that matrix A_0 is stable, one has

$$|\varepsilon_x| \leq \delta_\varepsilon \tag{18}$$

where δ_ε is a vector of unknown but bounded functions.

D. Output Differential Observer

The variables x_2 and $\dot{x}_2$ in the right-hand side of model (8) represent the angular velocity and acceleration of the servo mechanism, respectively. In the ideal case, x_2 and $\dot{x}_2$ can be computed by differentiating the output angel x_1. However, because the differential operator is sensitive to noise, the derivative of the output angle cannot be used directly. Therefore, the output differential observer [19] shown in (19) is used to estimate the angular velocity and acceleration

$$\begin{cases} \dot{\hat{\underline{x}}}_1 = \hat{\underline{x}}_2 + a_1(x_1 - \hat{\underline{x}}_1) \\ \dot{\hat{\underline{x}}}_2 = \hat{\underline{x}}_3 + a_2(x_1 - \hat{\underline{x}}_1) \\ \dot{\hat{\underline{x}}}_3 = a_3(x_1 - \hat{\underline{x}}_1). \end{cases} \tag{19}$$

Let x_1 be the input and $\hat{\underline{x}}_1$ be the output, the transfer function of the output differential observer is

$$\frac{\hat{\underline{x}}_1(s)}{x_1(s)} = \frac{a_1 s^2 + a_2 s + a_3}{s^3 + a_1 s^2 + a_2 s + a_3}. \tag{20}$$

The pole placement method can be used to adjust the bandwidth of (20), so that $\hat{\underline{x}}_1$ can track x_1 in any prescribed rate. Then, $\hat{\underline{x}}_2$ and $\hat{\underline{x}}_3$ will track x_2 and $\dot{x}_2$ with desired fast response, respectively.

E. Recursive Controller Design via DSC

The design combines the DSC method with the ARC design procedure. In the following, the unmeasurable state x_3 is replaced by its estimates and the estimation errors are handled by robust feedback to achieve a guaranteed robust performance.

Step 1: First, a dynamic surface is defined as

$$S_1 = \dot{e}_1 + k_p e_1 = x_2 - x_{2eq}, \quad x_{2eq} := \dot{x}_{1d} - k_p e_1 \tag{21}$$

where $e_1 = \dot{x}_1 - x_{1d}(t)$ is the output tracking error, k_p is any positive feedback gain. Since $G_s(s) = e_1(s)/S_1(s) = 1/(s + k_p)$ is a stable transfer function, if S_1 is small or converges to zero exponentially, the output tracking error e_1 will be small or converge to zero exponentially too. Differentiating (21) and noting (8), we have

$$\begin{aligned}\dot{S}_1 &= -\theta_1 x_2 + x_3 - \theta_2 S_f(x_2) + \Delta_1 - \dot{x}_{2eq} \\ &= \varphi_2^T \theta + \xi_{0,2} + \theta_6 \xi_{6,2} + \varepsilon_{x,2} + \Delta_1 - \dot{x}_{2eq}\end{aligned} \tag{22}$$

where $\varphi_2 = [\xi_{1,2} - x_2, \xi_{2,2} - S_f(x_2), \xi_{3,2}, \xi_{4,2}, \xi_{5,2}, 0]^T$. In the following, we use the ARC approach proposed in [2] to cope with the parametric uncertainties and uncertain nonlinearity Δ_1, $\varepsilon_{x,2}$ in (22). If the filter state $\xi_{6,2}$ were the actual control input, one could synthesize for it a virtual control law $\bar{\alpha}_2$ as follows:

$$\begin{cases} \bar{\alpha}_2 = \bar{\alpha}_{2a} + \bar{\alpha}_{2s}; \\ \bar{\alpha}_{2a} = \left(-\varphi_2^T \hat{\theta} - \xi_{0,2} + \dot{x}_{2eq}\right) / \hat{\theta}_6; \\ \bar{\alpha}_{2s} = \bar{\alpha}_{2s1} + \bar{\alpha}_{2s2} + \bar{\alpha}_{2s3}; \\ \bar{\alpha}_{2s1} = -k_{2s} S_1 / \theta_{6\min} \end{cases} \tag{23}$$

where $\bar{\alpha}_{2a}$ is the adaptive control term and $\bar{\alpha}_{2s}$ is the robust control term, k_{2s} is a positive design parameter. In (23), $\bar{\alpha}_{2s2}$ is selected to satisfy the following condition:

$$S_1(\Delta_1 + \theta_6 \bar{\alpha}_{2s2}) \le \varepsilon_{2,1} \tag{24}$$

and $\bar{\alpha}_{2s3}$ is any continuous function satisfying

$$S_1(\varepsilon_{x,2} + \theta_6 \bar{\alpha}_{2s3}) \le \varepsilon_{2,2} \delta_\varepsilon^2 \tag{25}$$

where $\varepsilon_{2,1}$ and $\varepsilon_{2,2}$ are positive parameters to be chosen. Introduce a new variable α_2 and let $\bar{\alpha}_2$ pass through a first-order filter with time constant τ_2 to obtain α_2

$$\tau_2 \dot{\alpha}_2 + \alpha_2 = \bar{\alpha}_2, \quad \alpha_2(0) = \bar{\alpha}_2(0). \tag{26}$$

Essentially, (24) shows that $\bar{\alpha}_{2s2}$ is synthesized to attenuate the effect of uncertain nonlinearities with known bound (i.e., Δ_1) to the level of control accuracy measured by $\varepsilon_{2,1}$. Similarly, it can be seen from (25) that $\bar{\alpha}_{2s3}$ is used to counteract the effect of state estimation error $\varepsilon_{x,2}$.

Step 2: The second dynamic surface is defined as

$$S_2 = \xi_{6,2} - \alpha_2. \tag{27}$$

From (15) and (23), the derivative of S_2 is

$$\dot{S}_2 = -k_2 \xi_{6,1} + u - (\bar{\alpha}_2 - \alpha_2)/\tau_2. \tag{28}$$

The control input u, which consists of two parts, is design as follows:

$$\begin{cases} u = u_a + u_s; \quad u_s = -k_{3s} S_2 \\ u_a = k_2 \xi_{6,1} + (\bar{\alpha}_2 - \alpha_2)/\tau_2 - \hat{\theta}_6 S_1 \end{cases} \tag{29}$$

where u_a is the adaptive control term; u_s is the robust control term.

Step 3: The adaptation law to update the parameter estimates is chosen as

$$\begin{cases} \dot{\hat{\theta}} = \mathrm{Proj}_{\hat{\theta}}(\Gamma\tau); \quad \tau = \varphi_a S_1; \\ \varphi_a = [\xi_{1,2} - x_2, \xi_{2,2} - S_f(x_2), \xi_{3,2}, \xi_{4,2}, \xi_{5,2}, S_2 + \bar{\alpha}_{2a}]^T. \end{cases} \tag{30}$$

Remark 1: One smooth example of $\bar{\alpha}_{2s2}$ satisfying (24) can be found in the following way. Let h_2 be any smooth function or constant satisfying

$$h_2 \ge \delta_1^2. \tag{31}$$

Then, $\bar{\alpha}_{2s2}$ can be chosen as [1], [2]

$$\bar{\alpha}_{2s2} = -\frac{h_2}{4\theta_{6\min}\varepsilon_{2,1}} S_1. \tag{32}$$

Similarly, an example of $\bar{\alpha}_{2s3}$ satisfying (25) is given by [20]

$$\bar{\alpha}_{2s3} = -\frac{1}{4\theta_{6\min}\varepsilon_{2,2}} S_1.. \tag{33}$$

Other smooth or continuous examples of $\bar{\alpha}_{2s2}$ and $\bar{\alpha}_{2s3}$ can be worked out in the same way as in [6]–[8].

IV. Stability Analysis of the Closed-Loop System

Define a scalar y_2 as

$$y_2 = \alpha_2 - \bar{\alpha}_2. \tag{34}$$

From (23) and (26), the derivative of y_2 is

$$\begin{aligned}\dot{y}_2 = -\frac{y_2}{\tau_2} + \frac{1}{\hat{\theta}_6}\Bigg(&\varphi_2^T \dot{\hat{\theta}} + \hat{\theta}^T \frac{\partial \varphi_2}{\partial x}\dot{x} + \hat{\theta}^T \sum_{i=1}^{5} \frac{\partial \varphi_2}{\partial \xi_{i,2}} \dot{\xi}_{i,2} \\ &+ \dot{\xi}_{0,2} - \ddot{x}_{2eq}\Bigg) - \frac{\partial \bar{\alpha}_{2s}}{\partial S_1}\dot{S}_1 + \frac{\dot{\hat{\theta}}_6}{\hat{\theta}_6}\bar{\alpha}_{2a}.\end{aligned} \tag{35}$$

All terms in (35) can be dominated by some continuous functions, therefore, we have

$$\left|\dot{y}_2 + \frac{y_2}{\tau_2}\right| \le B_2(S_1, S_2, y_2, \hat{\theta}, x_{1d}, \dot{x}_{1d}, \dot{x}_{1d}) \tag{36}$$

where B_2 is a continuous function. Then, the following inequality can be obtained:

$$y_2 \dot{y}_2 + \frac{y_2^2}{\tau_2} \le \left| y_2 \dot{y}_2 + \frac{y_2^2}{\tau_2} \right| \le B_2 |y_2|. \tag{37}$$

Thus

$$y_2 \dot{y}_2 \le -\frac{y_2^2}{\tau_2} + B_2 |y_2| \le -\frac{y_2^2}{\tau_2} + y_2^2 + \frac{1}{4} B_2^2. \tag{38}$$

From (22), (23), (27), (30), and (34), $\dot{S}_1$ can be derived as

$$\begin{aligned}\dot{S}_1 =& \varphi_2^T\theta + \xi_{0,2} + \theta_6(y_2 + \bar{\alpha}_2 + S_2) + \varepsilon_{x,2} + \Delta_1 - \dot{x}_{2eq} \\ =& -\varphi_a^T\tilde{\theta} - k_{2s}\frac{\theta_6}{\theta_{6\min}}S_1 + \varepsilon_{x,2} + \Delta_1 \\ &+ \theta_6(\bar{\alpha}_{2s2} + \bar{\alpha}_{2s3} + y_2) + \hat{\theta}_6 S_2. \end{aligned} \tag{39}$$

Then, we have

$$\begin{aligned}S_1\dot{S}_1 =& -k_{2s}(\theta_6/\theta_{6\min})S_1^2 - \varphi_a^T\tilde{\theta}S_1 + (\theta_6\bar{\alpha}_{2s2} + \Delta_1)S_1 \\ &+ (\theta_6\bar{\alpha}_{2s3} + \varepsilon_{x,2})S_1 + \theta_6 y_2 S_1 + \hat{\theta}_6 S_1 S_2 \\ \leq& -k_{2s}S_1^2 - \varphi_a^T\tilde{\theta}S_1 + \varepsilon_{2,1} + \varepsilon_{2,2}\delta_\varepsilon^2 \\ &+ \theta_{6\max}\left(S_1^2 + y_2^2\right)/2 + \hat{\theta}_6 S_1 S_2. \end{aligned} \tag{40}$$

From (28) and (29), it follows that

$$\dot{S}_2 = -\hat{\theta}_6 S_1 - k_{3s}S_2. \tag{41}$$

Then, we obtain

$$S_2\dot{S}_2 = -k_{3s}S_2^2 - \hat{\theta}_6 S_1 S_2. \tag{42}$$

Before the main result of stability is given, the sets and values which will be used in the stability proof are defined below. For any $p > 0$, define

$$\Pi = \left\{(S_1, S_2, y_2, \hat{\theta}) : V(t) \leq p\right\}$$

where

$$V(t) = \frac{1}{2}S_1^2 + \frac{1}{2}S_2^2 + \frac{1}{2}y_2^2 + \frac{1}{2}\tilde{\theta}^T\Gamma^{-1}\tilde{\theta}. \tag{43}$$

Obviously, Π is a compact subset in $\Re^9$, hence there must be a point corresponding to the supreme value of B_2 in Π. We denote this supreme value as M_2, that is

$$B_2 \leq M_2. \tag{44}$$

Theorem 1: Considering system (6), if the control law is (29), adaptation law is (30) and assumption $1 \sim 3$ are satisfied, then for any initial states in Π, there exist positive parameters k_{2s}, k_{3s}, τ_2, $\varepsilon_{2,1}$, and $\varepsilon_{2,2}$ satisfying

$$\begin{cases} k_{2s} - \frac{\theta_{6\max}}{2} \geq \alpha_0 \\ k_{3s} \geq \alpha_0 \\ \frac{1}{\tau_2} - 1 - \frac{\theta_{6\max}}{2} \geq \alpha_0 \\ \exists\alpha_0 > 0 \end{cases} \tag{45}$$

such that all signals of the closed-loop system are uniformly ultimately bounded and the steady-state tracking error can be made arbitrarily small.

Proof: Considering the positive definite function $V(t)$ in (43), from (30), (38), (40), and (42), the derivative of $V(t)$ can be found as follows:

$$\begin{aligned}\dot{V} =& S_1\dot{S}_1 + S_2\dot{S}_2 + y_2\dot{y}_2 + \tilde{\theta}\Gamma^{-1}\dot{\hat{\theta}} \\ \leq& -k_{2s}S_1^2 - \varphi_a^T\tilde{\theta}S_1 + \varepsilon_{2,1} + \varepsilon_{2,2}\delta_\varepsilon^2 + \hat{\theta}_6 S_1 S_2 \\ &+ \theta_{6\max}\frac{S_1^2 + y_2^2}{2} - k_{3s}S_2^2 - \hat{\theta}_6 S_1 S_2 - \frac{y_2^2}{\tau_2} + y_2^2 \\ &+ \frac{1}{4}B_2^2 + \tilde{\theta}\Gamma^{-1}\mathrm{Proj}_{\hat{\theta}}(\Gamma\varphi_a S_1). \end{aligned} \tag{46}$$

Noting (13) and (44), we have

$$\begin{aligned}\dot{V} \leq& -k_{2s}S_1^2 - \varphi_a^T\tilde{\theta}S_1 + \varepsilon_{2,1} + \varepsilon_{2,2}\delta_\varepsilon^2 + \hat{\theta}_6 S_1 S_2 \\ &+ \theta_{6\max}\frac{S_1^2 + y_2^2}{2} - k_{3s}S_2^2 - \hat{\theta}_6 S_1 S_2 - \frac{y_2^2}{\tau_2} \\ &+ y_2^2 + \frac{1}{4}M_2^2 + \tilde{\theta}^T\varphi_a S_1 \\ \leq& -\left(k_{2s} - \frac{\theta_{6\max}}{2}\right)S_1^2 - \left(\frac{1}{\tau_2} - 1 - \frac{\theta_{6\max}}{2}\right)y_2^2 \\ &- k_{3s}S_2^2 - \alpha_0\tilde{\theta}^T\Gamma^{-1}\tilde{\theta} + \frac{1}{4}M_2^2 + \varepsilon_{2,1} + \varepsilon_{2,2}\delta_\varepsilon^2 \\ &+ \alpha_0\tilde{\theta}^T\Gamma^{-1}\tilde{\theta}. \end{aligned} \tag{47}$$

Define a positive number R_0 satisfying

$$R_0 = \frac{1}{4}M_2^2 + \varepsilon_{2,1} + \varepsilon_{2,2}\delta_\varepsilon^2 + \alpha_0 M_\theta \tag{48}$$

where $M_\theta = (\theta_{\max} - \theta_{\min})^T\Gamma^{-1}(\theta_{\max} - \theta_{\min})$. Substituting (45) and (48) into (47) yields

$$\dot{V} \leq -2\alpha_0 V + R_0. \tag{49}$$

Let

$$\alpha_0 \geq R_0/(2p) \tag{50}$$

then $\dot{V} \leq 0$ on $V = p$. Thus, $V \leq p$ is an invariant set, i.e., if $V(0) \leq p$, then $V(t) \leq p$ for all $t \geq 0$. Therefore, $V(t)$ is bounded, so does S_1, S_2, y_2, and $\tilde{\theta}$.

Define a positive definite function V_n satisfying

$$V_n(t) = \frac{1}{2}S_1^2 + \frac{1}{2}S_2^2 + \frac{1}{2}y_2^2. \tag{51}$$

In order to made a contradiction, we assume that there exist $T > 0$, so that when $t > T$

$$V_n(t) > \frac{R}{2\alpha_0} + \varepsilon \tag{52}$$

where ε is an arbitrary positive number and R is given by

$$R = (1/4)M_2^2 + \varepsilon_{2,1} + \varepsilon_{2,2}\delta_\varepsilon^2. \tag{53}$$

From (45), (47), (51), and (53), we know that

$$\dot{V}(t) \leq -2\alpha_0 V_n + R. \tag{54}$$

Multiplying -1 to both sides of (54), yields

$$2\alpha_0 V_n - R \leq -\dot{V}. \tag{55}$$

Integrating (55) over $[0, t]$, we have

$$f(t) := \int_0^t 2\alpha_0 V_n(\tau) - R\mathrm{d}\tau \leq V(0) - V(t). \tag{56}$$

Due to the boundedness of $V(t)$ proven above, the function $f(t)$ is upper bounded. From (52) and (56), it can be seen that $f(t)$ is

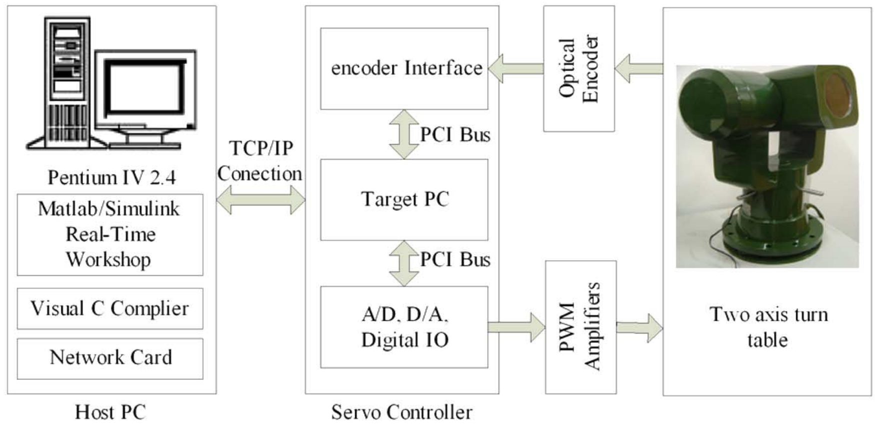

Fig. 1. Structure of the two-axis turntable servo system.

monotone increasing. Therefore, $f(t)$ has a finite limit as $t \to \infty$. The second-order derivative of $f(t)$ is

$$\ddot{f}(t) = 2\alpha_0 \dot{V}_n(t) - R = 2\alpha_0 (S_1 \dot{S}_1 + S_2 \dot{S}_2 + y_2 \dot{y}_2) - R. \quad (57)$$

Because of the boundedness of S_1, S_2, y_2, and $\tilde{\theta}$, together with (37), (40), (42), and (44), $\ddot{f}(t)$ is also bounded. According to the Barbalat's lemma, we obtain that

$$\lim_{t\to\infty} \dot{f}(t) = \lim_{t\to\infty} 2\alpha_0 V_n(t) - R = 0. \quad (58)$$

It is obvious that (58) contradicts with (52), hence we have

$$V_n(t) \le \frac{R}{2\alpha_0} + \varepsilon, \quad \forall t > T. \quad (59)$$

Note that ε can be chosen arbitrarily small. From (59), we know that y_2, S_1, and S_2 are uniformly ultimately bounded. Noting Property 2 and (12), it is obvious that $\tilde{\theta}$ is uniformly ultimately bounded. Furthermore, x_1, x_2, α_2, and $\hat{\theta}$ are also uniformly ultimately bounded. From (45) and (53), we can see that, for any given constants θ_{6max}, M_2, and δ_ϵ, R/α_0 can be made arbitrarily small by properly choosing k_{2s}, k_{3s}, τ_2, $\varepsilon_{2,1}$, and $\varepsilon_{2,2}$. This implies that the steady-state tracking error can be made arbitrarily small. □

Remark 2: In theorem 1, we investigated the systems with initial conditions satisfying $V(t) \le p$. It implies that all related variables must be in a ball of radius $\sqrt{2p}$ at the initial time. However, since p can be arbitrarily large, the condition $V(t) \le p$ is not really restrictive.

Remark 3: The inequality (45), (50), and (53) provide a guideline to tune the parameters k_{2s}, k_{3s}, τ_2, $\varepsilon_{2,1}$, and $\varepsilon_{2,2}$ for the designer. If k_{2s} and k_{3s} increase, or τ_2 decrease, then α_0 increase and R/α_0 is subsequently reduced. If $\varepsilon_{2,1}$ and $\varepsilon_{2,2}$ decrease, then R decrease and consequently R/α_0 is reduced, which leads to smaller tracking error for the system.

Remark 4: If adaptation is removed from the controller, i.e., $\Gamma = \mathrm{diag}[0,0,0,0,0,0]$, then from (45) and (46) we know that

$$\begin{aligned}\dot{V}_n \le & -\left(k_{2s} - \frac{\theta_{6\max}}{2}\right) S_1^2 - k_{3s} S_2^2 \\ & - \left(\frac{1}{\tau_2} - 1 - \frac{\theta_{6\max}}{2}\right) y_2^2 \\ & + \frac{1}{4} M_2^2 + \varepsilon_{2,1} + \varepsilon_{2,2}\delta_\varepsilon^2 - \varphi_a^T \tilde{\theta} S_1 \\ \le & -2\alpha_0 V_n + R - \varphi_a^T \tilde{\theta} S_1. \end{aligned} \quad (60)$$

The last term of the right-hand side of (60), i.e.,$-\varphi_a^T \tilde{\theta} S_1$, which may steer V_n to infinity, can be regarded as the influence of parameter uncertainties. For ARC, this deleterious effect could be completely cancelled by the adaptive control term. From (60), we know that if $\tilde{\theta} = 0$ the controller without adaptation is still able to achieve ultimately uniform boundedness. Actually, the first two design steps of the proposed ARC are coherent with the design procedures of a deterministic dynamic surface controller (DDSC) for plants with partial unknown states. In the following section, the proposed ARC and the DDSC will be investigated and compared by experiments.

V. Experimental Results and Analysis

A. Experimental Setup

To demonstrate the effectiveness of the proposed ARC, a two-axis turntable servo system is set up as a test-bed. As shown in Fig. 1, the test-bed consists of five major components: a two-axis turntable, optical encoder, PWM amplifiers, a servo controller, and a host PC. The resolution of the optical encoder is 0.0005 degree. The two axes of the turntable (i.e., yaw axis and pitch axis) are mounted orthogonally. They are driven by two dc torque motors. respectively.

The controller of the servo mechanism is implemented through an Xpc target that consists of a target personal computer and the interface card NI PCI-6052E. The sampling rate of the servo controller is 2 kHz, a value in common use for servo mechanisms.

B. Design of the Controllers

In the experiments, only yaw axis is used. Model (8) is utilized to describe the dynamics of the yaw axis. Identification is performed to obtain the parameters, whose values are shown in Table I. According to (10), the parameters of model (8) can be computed, and then we have: $\theta = [9.091, 52.4, 1095, 98.04, 5133.7, 11337]^T$. The bounds of the parameters can be chosen as $\theta_{\min} = [5, 50, 1000, 80, 5000, 10000]^T$; $\theta_{\max} =$

TABLE I
PARAMETERS OF THE YAW AXIS

Parameters	Quantities
J(kg·m^2)	0.011
R(Ω)	5.0
L(H)	0.051
θ_f(N)	0.576
K_F(N/A)	6.36
K_E(V/m/s)	0.018
B(N/m/s)	0.1

$[12, 60, 1200, 100, 6000, 13000]^T$. According to the parameters of the plant model, the following two controllers are design.

1) Adaptive Robust Controller (ARC): Based on the design procedures introduced in Section III, the controller is designed as follows. All the roots of the state observer eigenvalue polynomial are placed at $s = -200$, which leads to $k_1 = 400$ and $k_2 = 40\,000$. The parameter K_s in the approximating function S_f is chosen as $K_s = 900$. As mentioned in Remark 3, if the controller parameters k_p, k_{2s}, and k_{3s} are increased, or the parameters τ_2, $\varepsilon_{2,1}$, and $\varepsilon_{2,2}$ are reduced, the tracking error will be decreased and the transient response would be accelerated. However, every physical plant has a bandwidth limit and saturation nonlinearities. If the parameters k_p, k_{2s}, and k_{3s} are too large, the system may be suffered from the saturation nonlinearities and bandwidth limit. On the other hand, if the parameters τ_2, $\varepsilon_{2,1}$, and $\varepsilon_{2,2}$ are too small, the system might be excessively sensitive to noise. With consideration of these issues, we tune the parameters of ARC, and obtain the following parameter values: $k_p = 50$, $k_{2s} = 500$, $k_{3s} = 300$, $\tau_2 = 0.2$, $\varepsilon_{2,1} = 0.005$, $\varepsilon_{2,2} = 0.005$, and $h_2 = 1$, where h_2 is corresponding to the level of disturbance as stated in Remark 1. The adaptation rate is chosen as $\Gamma = \mathrm{diag}[5, 50, 100, 10, 100, 500]$. The initial parameter estimates are $\hat{\theta}(0) = [5, 50, 1000, 80, 5000, 10000]^T$. All the poles of the output differential observer are placed at -100, so that we obtain $a_1 = 300$, $a_2 = 3\times 10^4$, $a_3 = 1\times 10^6$.

2) Deterministic Dynamic Surface Controller (DDSC): The same control law as the ARC designed previously but without adaptation, i.e., letting $\Gamma = \mathrm{diag}[0, 0, 0, 0, 0, 0]$.

For engineering applications, the ARC is more complicated than the DDSC in computation, because the ARC utilizes adaptation law which is not used in the DDSC. However, the adaptation law enables the ARC to achieve more favorable tracking performance than the DDSC as is shown in the following experimental results.

C. Experimental Results

In order to compare the two controllers in quantity, the following performance indices will be used [21], [22].

(I1) $L_2[e] = \sqrt{(1/T_f)\int_0^{T_f} |e(t)|^2 dt}$, the L_2 norm of the tracking error, is used as a measure of average tracking performance, where T_f represents the total running time.

(I2) $e_M = \max_t |e(t)|$, the maximum absolute value of the tracking error, is used as a measure of transient performance.

TABLE II
TRACKING PERFORMANCE FOR THE 1 Hz SINUSOIDAL TRAJECTORY

Controllers	e_M(deg)	$L_2[e]$ (deg)	e_F (deg)
(set 1) ARC	0.0123	0.00803	0.00859
(set 1)DDSC	0.0171	0.0107	0.0170
(set 2) ARC	0.0164	0.00881	0.0143
(set 2)DDSC	0.0187	0.0116	0.0172

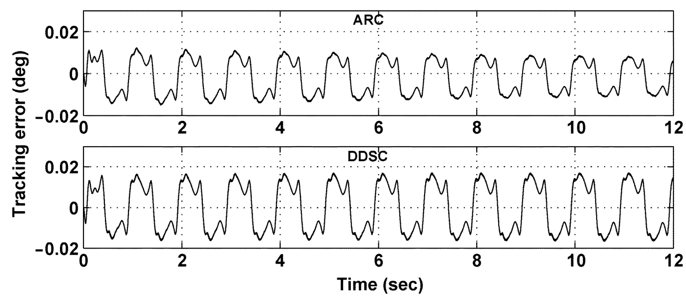

Fig. 2. Tracking errors for sinusoidal trajectory $x_d = 10\sin(2\pi t)$.

(I3) $e_F = \max_{T_f-2T\le t\le T_f} |e(t)|$, the maximum absolute value of the tracking error during the last two periods of the experiment, is used as a measure of final tracking accuracy for periodic trajectories with a period T.

1) Case 1: Since the influence of friction nonlinearity, disturbance (ripple torque) and sensor noises is more notable at low speed, to test the robustness of the controllers, we just let the yaw axis track a slow sinusoidal signal in this case. The desired trajectory is selected to be $x_d = 10\sin(2\pi t)$, which means a sinusoidal input with an amplitude of 10 degree and a frequency of 1 Hz. The following test sets are performed.

Set 1) The yaw axis tracks the slow sinusoidal trajectory without external disturbance added.

Set 2) To further verify the robustness to the external disturbance, an electrical signal $0.2\sin(2\pi t)$ (V) is added to the control input. We just use this electrical signal to simulate a sinusoidal disturbance torque added to the yaw axis.

The experimental results in terms of performance indices are given in Table II. As seen, ARC achieves a better tracking performance than DDSC, since all the indices (i.e., e_M, $L_2[e]$, and e_F) of ARC are less than those of DDSC.

For Set 1, the tracking errors are shown in Fig. 2. It shows that the tracking error of ARC decrease gradually due to adaptation, while the DDSC has a larger tracking error with constant magnitude. The parameter estimates are shown in Fig. 3. It can be seen that the parameter estimates never run out of the prescribed bound for the use of projection operator. There is no guarantee that the parameter estimates will converge to their true values, because our trajectories do not usually provide enough persistent excitation and the adaptation is very slow when error is too small. Although parameter estimates do not necessarily converge to their values, as seen from Remark 4 and Fig. 2, the parameter adaptation is able to cancel the adverseness of parameter uncertainties and improve the tracking performance. For Set 2, the tracking errors are given in Fig. 4. As we can see, the added sinusoidal disturbance does not affect the performance of ARC much. That is because the robust control term of ARC can attenuate the influence of external disturbance effectively.

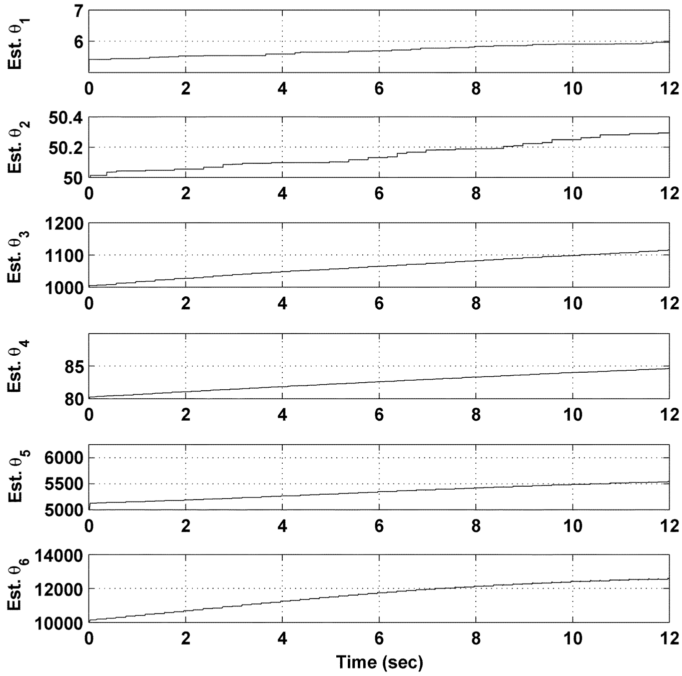

Fig. 3. Parameter estimation of ARC under sinusoidal excitation.

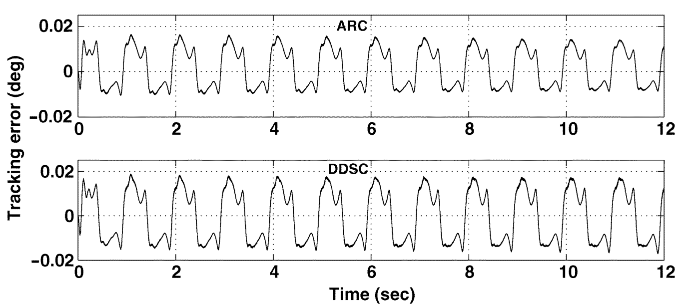

Fig. 4. Tracking errors for sinusoidal trajectory $x_d = 10\sin(2\pi t)$ under the influence of added disturbance.

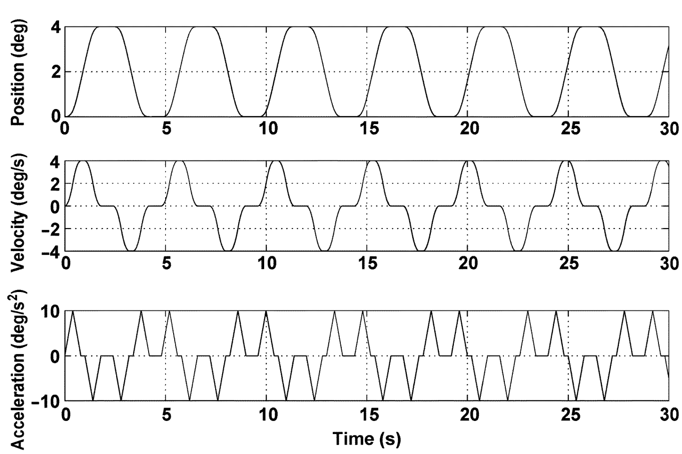

Fig. 5. Point-to-point motion trajectory.

2) Case 2: To demonstrate the tracking performance, the test-bed is then commanded to track a point-to-point motion trajectory shown in Fig. 5. Following this trajectory, the yaw axis of the turntable will rotate clockwise and counter clockwise between the position of 0 degree and the position of 4 degree, with a top velocity of ± 4 deg/s and a top acceleration of ± 10 deg/s^2. The tracking errors of both controllers are shown in Fig. 6. The performance indices are given in Table III, which demonstrates that the ARC has better tracking performance than the DDSC. That is because of the parameter adaptation of ARC, which is shown in Fig. 7. As seen, the parameter estimates are within the prescribed bound owning to the projection operator. In this case, parameter adaptation appears faster than that of Case 1 for a better excitation of point-to-point trajectory.

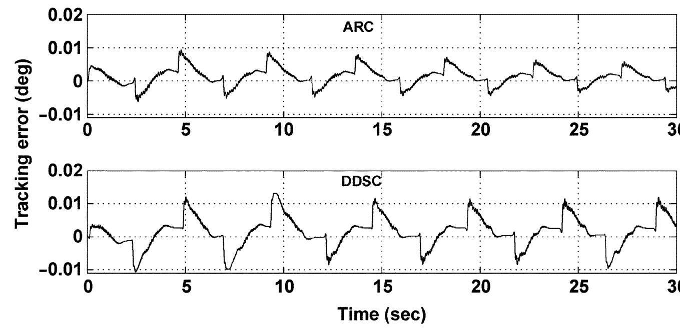

Fig. 6. Tracking error of point-to-point trajectory.

TABLE III
TRACKING PERFORMANCE FOR THE POINT-TO-POINT TRAJECTORY

Controllers	e_M(deg)	$L_2[e]$(deg)	e_F (deg)
ARC	0.00931	0.00291	0.00630
DDSC	0.0131	0.00472	0.0119

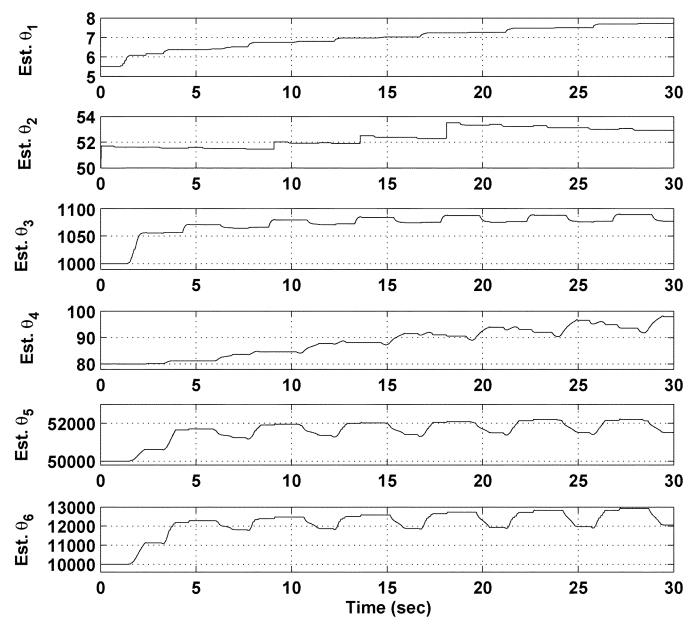

Fig. 7. Parameter adaptation under point-to-point trajectory excitation.

VI. CONCLUSION

In this paper, an ARC scheme based on state observer was presented for the servo mechanisms with unknown states, parametric uncertainties and disturbances. The problem of "explosion of complexity", which usually exists in the ARC designed by traditional backstepping approach, is overcome by dynamic surface control technique. The proposed ARC utilizes parameter adaptation to eliminate the influence of parametric uncertainties and uses robust control terms to attenuate the influence of disturbances. It was proved that all signals in the closed-loop system are uniformly ultimately bounded, and that the tracking error can be made arbitrarily small by adjusting the parameters in the control law. In addition, the theoretical-analysis results were verified through experimental results. Future work will be focused on the extension of the proposed ARC to the multi-objective control [23].

REFERENCES

[1] B. Yao, "High performance adaptive robust control of nonlinear systems: A general framework and new schemes," in *Proc. 36th IEEE Conf. Dec. Control*, San Diego, 1997, pp. 2489–2494.

[2] B. Yao and M. Tomizuka, "Adaptive robust control of SISO nonlinear systems in a semi-strict feedback form," *Automatica*, vol. 33, no. 5, pp. 893–900, 1997.

[3] M. Kristic, Kanellakopoulos, and P. V. Kokotovic, *Nonlinear and Adaptive Control Design*. New York: Wiley, 1995.

[4] V. I. Utkin, *Sliding Modes in Control Optimization*. Berlin, Germany: Springer-Verlag, 1992.

[5] B. Yao, "Adaptive robust control: Theory and applications to integrated design of intelligent and precision mechatronic systems," in *Proc. Int. Conf. Intell. Mechatron. Autom.*, Chengdu, China, 2004, pp. 35–40.

[6] L. Xu and B. Yao, "Adaptive robust motion control of linear motors for precision manufacturing," *Mechatronics*, vol. 12, no. 4, pp. 595–616, 2002.

[7] Z.-J. Yang and K. Kunitoshi, "Adaptive robust output-feedback control of a magnetic levitation system by K-filter approach," *IEEE Trans. Ind. Electron.*, vol. 55, no. 1, pp. 390–399, Jan. 2008.

[8] L. Xu and B. Yao, "Output feedback adaptive robust precision motion control of linear motors," *Automatica*, vol. 37, no. 7, pp. 1029–1039, 2001.

[9] J. A. Farrell, M. Polycarpou, M. Sharma, and W. Dong, "Command filtered backstepping," in *Proc. Amer. Control Conf.*, Seattle, WA, 2008, pp. 1923–1928.

[10] D. Swaroop, J. K. Hedrick, and P. P. Yip, "Dynamic surface control for a class of nonlinear systems," *IEEE Trans. Autom. Control*, vol. 45, no. 10, pp. 1893–1899, Oct. 2000.

[11] D. Wang and J. Huang, "Neural network-based adaptive dynamic surface control for a class of uncertain nonlinear systems in strict-feedback form," *IEEE Trans. Neural Netw.*, vol. 16, no. 1, pp. 195–202, Jan. 2005.

[12] T. P. Zhang and S. S. Ge, "Adaptive dynamic surface control of nonlinear systems with unknown dead zone in pure feedback form," *Automaica*, vol. 44, no. 7, pp. 1895–1903, 2008.

[13] Z. Yang, T. Nagai, S. Kanae, and K. Wada, "Dynamic surface control approach to adaptive robust control of nonlinear systems in semi-strict feedback form," *Int. J. Syst. Sci.*, vol. 38, no. 9, pp. 709–724, 2007.

[14] C. Canudas de Wit, H. Olsson, K. J. Astrom, and S. Lischinsky, "A new model for control of systems with friction," *IEEE Trans. Autom. Control*, vol. 40, no. 3, pp. 419–425, Mar. 1995.

[15] P. C. Krause, O. Wasynczuk, and S. D. Sudhoff, *Analysis of Electric Machinery*. New York: McGraw-Hill, 1986.

[16] L. Xu and B. Yao, "Observer based adaptive robust control of a class of nonlinear systems with dynamic uncertainties," in *Proc. 38th Conf. Dec. Control*, Phoenix, AZ, 1999, pp. 72–77.

[17] G. C. Goodwin and D. Q. Mayne, "A parameter estimation perspective of continuous time model reference adaptive control," *Automatica*, vol. 23, no. 1, pp. 57–70, 1989.

[18] B. Yao and M. Tomizuka, "Smooth robust adaptive sliding mode control of robot manipulators with guaranteed transient performance," in *Proc. Amer. Control Conf.*, 1994, pp. 1176–1180.

[19] X. Zhu, G. Tao, B. Yao, and J. Cao, "Adaptive robust posture control of a parallel manipulator driven by pneumatic muscles," *Automatica*, vol. 44, no. 9, pp. 2248–2257, 2008.

[20] B. Yao and L. Xu, "Output feedback adaptive robust control of uncertain linear systems with disturbances," *Trans. ASME, J. Dyn. Syst., Meas., Control*, vol. 128, no. 4, pp. 938–945, 2006.

[21] L. Xu and B. Yao, "Adaptive robust precision motion control of linear motors with negligible electrical dynamics: Theory and experiments," *IEEE Trans. Mechatronics*, vol. 6, no. 4, pp. 444–452, Apr. 2001.

[22] J. Zhong and B. Yao, "Adaptive robust precision motion control of a piezoelectric positioning stage," *IEEE Trans. Control Syst. Technol.*, vol. 16, no. 5, pp. 1039–1047, Sep. 2008.

[23] Z. Wang, H. Zeng, D. W. C. Ho, and H. Unbehauen, "Multi-objective control of a four-link flexible manipulator: A robust H_∞ approach," *IEEE Trans. Control Syst. Technol.*, vol. 10, no. 6, pp. 866–875, Nov. 2002.